A systematic study of solution and processing parameters on nanofiber morphology using a new electrospinning apparatus

Article *in* Journal of Nanoscience and Nanotechnology · July 2009

DOI: 10.1166/jnn.2009.NS27 · Source: PubMed

CITATIONS
34

READS
1,024

5 authors, including:

Célia Henriques
Universidade NOVA de Lisboa
25 PUBLICATIONS **375** CITATIONS

SEE PROFILE

Ricardo Vidinha
Medacta International SA
2 PUBLICATIONS **72** CITATIONS

SEE PROFILE

David Botequim
University of Lisbon
9 PUBLICATIONS **135** CITATIONS

SEE PROFILE

J.P. Borges
Faculty of Science and Technology New University of Lisbon
88 PUBLICATIONS **1,362** CITATIONS

SEE PROFILE

Journal of
Nanoscience and Nanotechnology
Vol. 8, 1–11, 2008

A Systematic Study of Solution and Processing Parameters on Nanofiber Morphology Using a New Electrospinning Apparatus

C. Henriques[1,*], R. Vidinha[1], D. Botequim[1], J. P. Borges[2], and J. A. M. C. Silva[1]

[1] *Physics Department, CeFITec, Faculty of Science and Technology, New University of Lisbon 2829-516 Caparica, Portugal*
[2] *Materials Science Department, CENIMAT/I3N Faculty of Science and Technology, New University of Lisbon 2829-516 Caparica, Portugal*

We assembled a new electrospinning apparatus and used poly(ethylene oxide) as a model polymer to perform a systematic study on the influence of solution and processing parameters on the morphology of electrospun nanofibers. Solution parameters studied were polymer concentration and molecular mass. The solvent used, 60 wt% water, 40 wt% ethanol, was the same throughout the study. Processing parameters analyzed were: solution feed rate, needle tip-collector distance and electrostatic potential difference between the needle and collector. Solution viscosity increased both with polymer concentration and molecular mass. Polymer concentration plays a decisive role on the outcome of the electrospinning process: a low concentration led to the formation of beaded fibers; an intermediate concentration yielded good quality fibers; a high concentration resulted in a bimodal size distribution and at even higher concentration a distributed deposition. Fiber diameter increased with polymer molecular mass and higher molecular masses are associated with a higher frequency of splaying events. Fiber diameter increased linearly with solution feed rate. While an increase in needle-collector distance represents a weaker electric field, a greater distance to be covered by the fibers and a longer flight time, presumably favoring the formation of thinner fibers, as solvent evaporation leads to a local increase of concentration and viscosity, viscoelastic forces opposing stretching caused an increase of fiber diameter with needle-collector distance. A higher voltage applied at the needle is associated with a higher charging of the polymer and a higher electrical current through it ultimately leading to incomplete solvent evaporation and merged fibers being produced. Controlling the charging of the polymer independently of the electric field strength was achieved by applying a voltage to the collector while distance and potential difference were kept constant. The increased electrostatic repulsion associated with an increase of the high voltage applied to the needle led to the disappearance of merged fibers.

Keywords: Electrospinning, Nanofibers, Poly(ethylene oxide), Viscosity, Non-Woven Mats.

RESEARCH ARTICLE

1. INTRODUCTION

A nanofiber is an elongated and threadlike structure with a diameter in the nanometre range. Nanofibrous mats have high porosity, small pore sizes and a high surface area. Electrospinning has the unique ability of producing nanofibers of different materials, with a good control of the fiber dimensions, in a scalable and cost-effective way.[1,2] Potential applications of electrospun nanofibers are manifold, with special emphasis in healthcare: as scaffolds for tissue engineering,[3–5] in wound dressing,[6–8] as vectors for the controlled release of drugs.[9–11]

Bead-free nanofibers of poly(ethylene oxide), PEO, are relatively easy to produce by electrospinning.[12–15] It is therefore a good model polymer to characterize a new electrospinning system. The objective of this work is to use our system to systematize and complement results found in the literature about PEO electrospinning[12–15] by studying the influence of solution and processing parameters on the morphological properties of the electrospun nanofiber mats.

Electrospinning involves electrically charging a polymer solution. In our assembly (see Fig. 1), the polymer solution is contained in an horizontal plastic syringe fitted with a metallic blunt tip needle held at high voltage. An advancement pump is used to control the polymer solution feed

*Author to whom correspondence should be addressed.

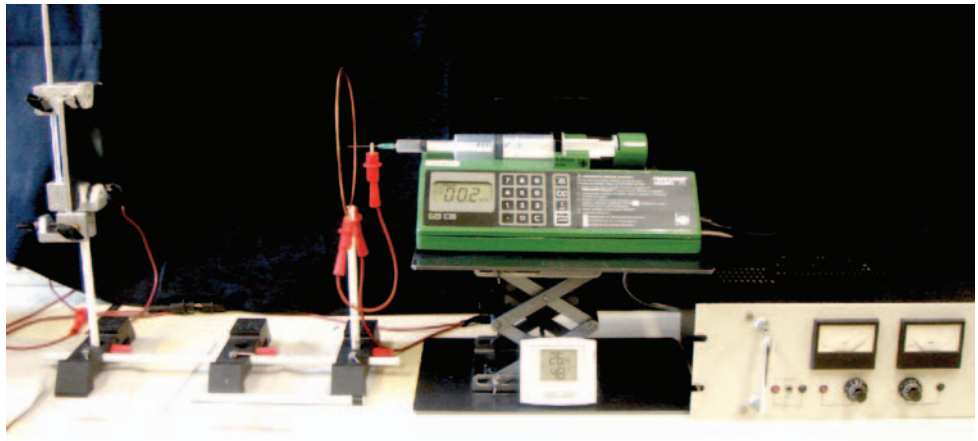

Fig. 1. Experimental set up (for a description see text).

rate. A metallic ring held vertical, with the needle tip at its center and electrically connected to the needle, improves the electric field configuration in such a way that facilitates the electrospinning process: in the needle tip region the ring causes a less intense field strength and the field lines tend to align in the direction parallel to the needle. Several forces competing during the electrospinning process can be identified: the electrostatic force acting on the charged jet due to the electric field between the needle and the collector; the coulombic electrostatic repulsion between adjacent charged elements within the jet which is responsible for stretching; viscoelastic forces and surface tension which act against stretch.

The charging of the polymer causes the formation of a hyperbolic conical shape known as Taylor cone.[16] When the repulsive electrostatic force overcomes the surface tension of the solution, a jet erupts from its tip. Preserving the Taylor cone requires a delicate balance between the feed rate and the electrostatic extraction rate. If the extraction rate, which depends on the high voltage applied to the needle and the tip-collector distance, is too low, the solution accumulates at the tip and the jet emerges from an ever increasing droplet. If the feed rate is too low, the Taylor cone collapses and the surface from which the jet erupts recedes into the needle. If the voltage is not too high, the jet continues to flow from the needle without interruptions; this is the most frequent situation.

A linear flow region near the tip of the needle is usually observed. Its length depends on the electrospinning conditions and, even for fixed conditions, it oscillates due to instabilities in the ratio between the flow and extraction rates. The linear region is sometimes very short and under certain conditions the jet splits or splays. Some control of these instabilities may be reached by adjustment of the feed rate and applied voltage.

As the charged jet accelerates toward regions of lower potential, the solvent gradually evaporates. The end of the linear region is marked by the onset of a bending and whipping process due to the auto-repulsion of the charged jet.[17] As a consequence of these processes, the jet elongates and narrows becoming very thin and invisible. The entanglements of the polymer chains prevent the jet from breaking up and the result is a nanofiber, which is then collected on a grounded aluminum foil held vertical. A typical deposition at the collector is displayed in Figure 2. The characteristics of the electrospun nanofiber mat depend on the polymer and solvent used as well as on the experimental conditions, like polymer solution feed rate, needle tip-collector distance and high voltage applied between needle and collector.

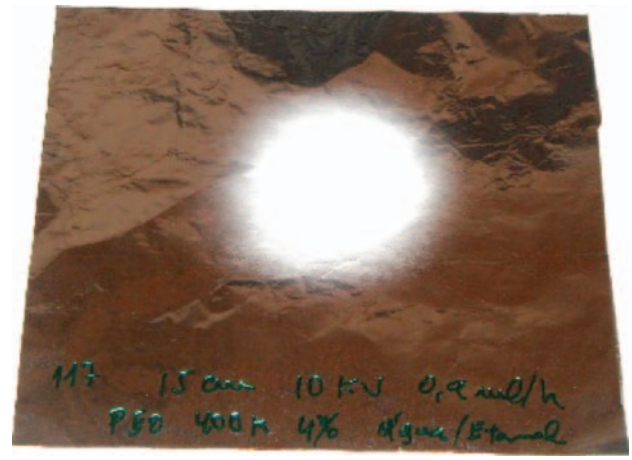

Fig. 2. Typical deposition on the collector.

2. MATERIALS AND METHODS

In this work we used poly(ethylene oxide) supplied by Sigma-Aldrich with average molecular masses of 400 kg/mol, 900 kg/mol, 2000 kg/mol, 5000 kg/mol and 8000 kg/mol. The polymer solutions were prepared by dissolving the PEO powder on a binary solution of water/ethanol mixed at a ratio of 3:2. The use of ethanol, a volatile solvent, improves the evaporation of the solvent from the fibers while they travel towards the collector,

RESEARCH ARTICLE

increases the viscosity and decreases the surface tension of the solution thereby facilitating the production of non-beaded fibers.[12] Solutions were mixed with a magnetic stirrer for several hours until complete dissolution. The viscosities of the solutions were determined with a rotational rheometer.

An advancement pump (B. Braun Perfusor secura FT) was used to control the polymer solution feed rate. The polymer solution was loaded into a 5 ml syringe with a 21-gauge needle attached. This syringe was placed inside a 60 ml syringe, the standard for the pump used. Therefore, the ratio between the true flow rates used and those selected on the pump is the ratio of the syringe internal sections.

A ring, with 15 cm of diameter, held vertical with the needle tip at its center was directly connected to the positive output of a high-voltage supply by an alligator clip. A cable with two alligator ends connected the ring to the needle.

Morphological characterization of the nanofibers (including fiber diameter distributions) was performed using scanning electron microscopy. Images of the electrospun nanofiber mats were obtained with a Zeiss (model DSM 962) SEM. All samples were sputter-coated with gold before SEM observation. Statistical diameter distributions were obtained from the SEM images.

3. RESULTS AND DISCUSSION

The influence of independent parameters on the morphology of fibers electrospun from PEO solutions was investigated. Processing parameters considered were the solution feed rate, the distance between the tip of the needle and the collector and the high voltage applied between the needle and the collector. Parameters of the polymer solution, namely the molecular mass of the polymer and the polymer concentration, were also considered. These two parameters, together with the solvents used, determine the viscosity of the solution.

Although viscosity is not an independent solution parameter it is frequently related to the spinnability of a polymer solution. The viscosity has been associated with the initial droplet shape and jet trajectory. Low viscosity solutions are unspinnable because the jet breaks up into droplets as a result of the high electrostatic repulsion needed to overcome the surface tension. Surface tension is

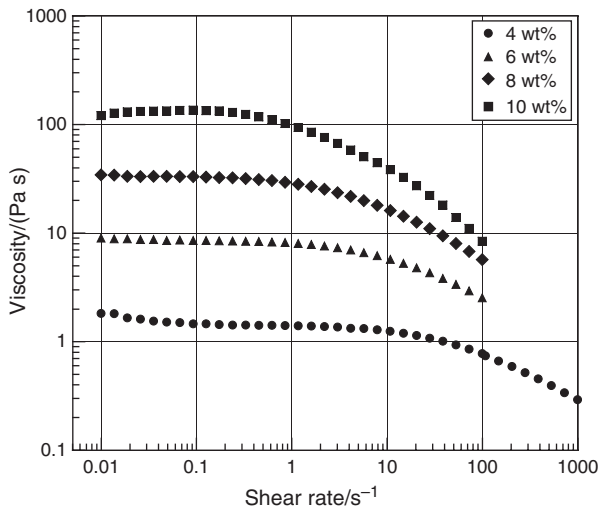

Fig. 3. Viscosities of the 400 kg/mol PEO solutions as a function of the shear rate. The zero shear viscosities found for the solutions with concentrations of 4 wt%, 6 wt%, 8 wt% and 10 wt% were, respectively, 1.5 Pa s, 8.7 Pa s, 33 Pa s and 136 Pa s.

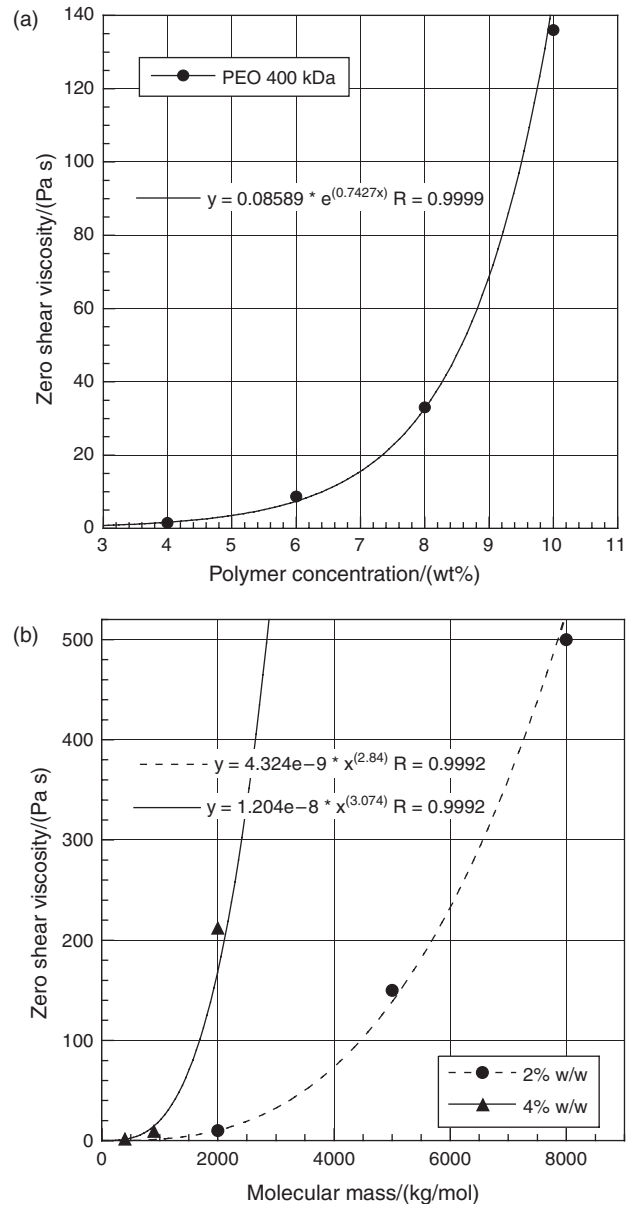

Fig. 4. Zero shear viscosity as a function of (a) polymer concentration and (b) molecular mass. Solid lines are fits (equations are displayed in the plots) which describe well the dependencies evidenced by the experimental data.

RESEARCH ARTICLE

another important solution dependent parameter but it is less sensitive to solution parameters than viscosity.[12]

The shear viscosities of the PEO stock solutions were measured at 25 °C, in a shear range of $10^{-2} - 10^{3}$ s^{-1} using a Bohlin (Gemini HR^{nano}) rotational rheometer equipped with 40 mm cone and plate fixtures. Prior to measuring the shear behavior, a preshear was applied to the samples in order to ensure a steady state. All solutions present a shear-thinning behavior as is shown in Figure 3 for the case of 400 kg/mol PEO solutions with concentrations in the range of 4% to 10%.

The shear viscosity increases with both PEO concentration and molecular mass. As can be seen from Figure 4(a), for the same polymer-solvent used the zero shear viscosity (hereby referred to simply as viscosity) increases very rapidly with the polymer concentration in the solution as the exponential fit to the experimental results evidences. Figure 4(b) shows that for a given concentration of polymer, the viscosity of the solution is also strongly dependent on the polymer molecular mass. Solutions with the same viscosity obtained from different molecular masses are reached at different concentrations: a higher molecular mass will require a smaller concentration. For a given molecular mass there is a spinnable concentration range which narrows with an increasing molecular mass.[18]

3.1. Polymer Concentration

PEO with an average molecular mass of 400 kg/mol was used to prepare solutions with different concentrations: 4 wt%, 6 wt%, 8 wt% and 10 wt%. The tip-collector distance was fixed at 20 cm.

Figure 5 shows SEM images of fiber mats obtained with an applied voltage of 10 kV and a feed rate of 0.1 ml/h. Fibers obtained from the 4 wt% solution contain elongated beads due to the low solution viscosity and high surface tension as pointed out by Fong et al.[12] The 6 wt% and 8 wt% solutions gave rise to fibers with the diameter distributions displayed in Figures 6(a) and (b), respectively. The distribution corresponding to the 6 wt% solution has a mean value of 258 nm. The width of the diameter

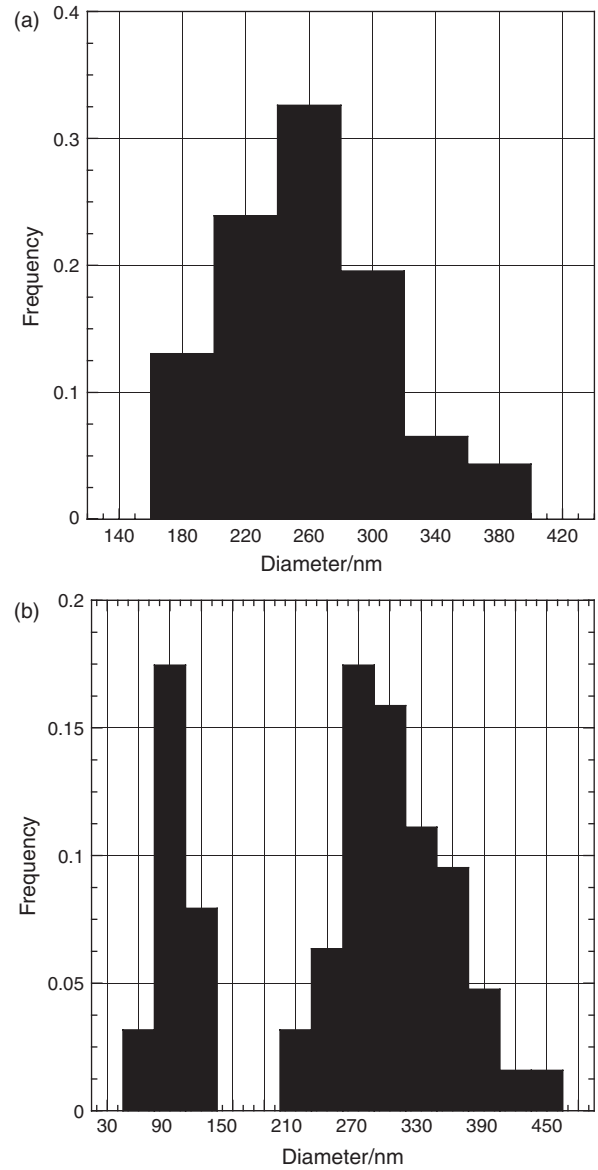

Fig. 6. Fiber diameter distributions for the (a) 6 wt% and (b) 8 wt% concentration 400 kg/mol PEO solutions.

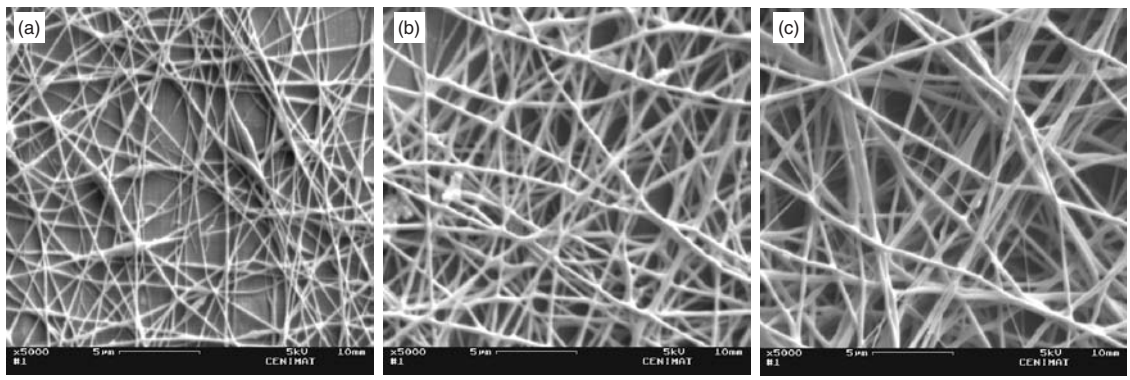

Fig. 5. Fibers electrospun from PEO solutions with different polymer concentrations: (a) 4 wt%, (b) 6 wt% and (c) 8 wt%.

RESEARCH ARTICLE

distribution, as measured by the experimental standard deviation, is 53 nm. The fibers obtained from the 8 wt% solution exhibit a bimodal distribution despite the fact that the deposition had the typical aspect displayed in Figure 2: Its two sub-distributions have mean values of (310 ± 52) nm and (94 ± 16) nm corresponding respectively to a principal and a secondary population of fibers (indicated uncertainties are standard deviations).

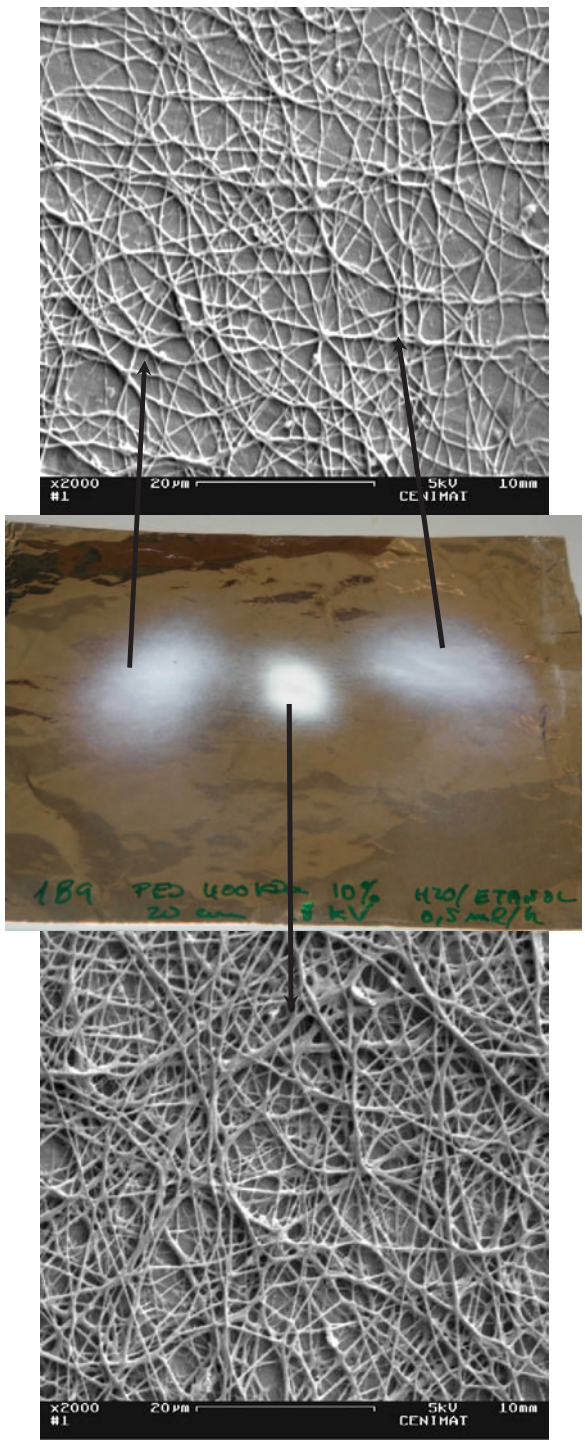

Fig. 7. Results of the electrospinning of a 10 wt% solution with its two distinct regions.

A bimodal distribution was previously reported for the electrospinning of 400 kg/mol PEO dissolved in water at 8 wt% and above[13] and it was attributed to splay events. These events were also observed to occur along the linear region of the jet in the electrospinning of our 8 wt% solution with water/ethanol as solvent.

When the concentration was increased to 10 wt%, keeping all processing parameters the same was not feasible: the jet initiation didn't occur due to a hight viscosity of the solution. An increase of the applied voltage to 18 kV, keeping the feed rate (0.1 ml/h) and the distance (20 cm) constants, led to a distributed deposition: three distinct regions could be seen on the collector (Fig. 7). The central region originates from a single jet emerging from a droplet formed at the needle tip. The high voltage used leads to the deposition of fibers with many defects as seen in Figure 7. The study on the influence of the high voltage on the morphology of the fibers is presented below. The high voltage used here (18 kV) also causes the highly charged single jet to split into two jets. These two jets emerge from the drop present at the needle tip.

The mutual repulsion of the two charged jets leads to the deposition of fibers in two satellite regions which consist of two symmetric lobes. Fibers in these outer regions have smaller diameters and present less defects than those in the central region. The two jets would eventually merge and deposition takes place again in the central region. These two deposition modes occur in alternating sequence. When both voltage and feed rate were lowered, to 15 kV and 0.05 ml/h, the drop was not formed and only one deposition area was observed. The corresponding fiber mat was also composed of fibers with a bimodal diameter distribution as the one observed for the 8 wt% solution case showing that the appearance of bimodal size distributions depend both on the polymer concentration and processing conditions.

3.2. Molecular Mass of the Polymer

The molecular mass is determined by the length of the polymeric chains. PEO is commercially available in a wide range of molecular masses: we used PEO with average molecular masses of 400 kg/mol, 900 kg/mol, 2000 kg/mol, 5000 kg/mol and 8000 kg/mol. Values for the different parameters were chosen so that acceptable electrospinning conditions could be achieved while most values, other than the molecular mass, were kept constant. Solution and processing parameters as well as the mean fiber diameters (in case of a bimodal distribution only the diameters of the thicker fibers were measured) are presented in Table I.

From the SEM images of Figures 8(a to c) we can conclude that a high molecular mass favors the formation of

Table I. Processing conditions and influence of molecular mass on mean fiber diameter of electrospun PEO fibers.

Molecular mass (kg/mol)	Concentration (wt%)	Potential (kV)	Tip-collector distance (cm)	Feed rate (ml/h)	Mean fiber diameter (nm)	Standard deviation in diameter (nm)
400	4	8	25	0.1	161 (beaded)	38
900	4	10	25	0.1	261	73
2000	4	10	25	0.1	453	61
2000	2	10	30	0.05	242	57
5000	2	10	30	0.05	701	139
8000	2	10	30	0.05	827	191

defect free fibers (see above discussion about the solution viscosity). However, considering images (d) to (f) we can see that when the molecular mass is further increased very thin fibers start to appear together with fibers of increasing diameter. The thin fibers are discontinuous either because they break after deposition or they result from an intermittent jet splitting or splaying, a phenomenon which was frequently observed for the highest molecular masses. With all other independent parameters fixed, the mean fibers resulting from the main continuous jet increases with the molecular mass as the graphic of Figure 9(a) shows. As viscosity and molecular mass are strongly correlated we plotted the mean fiber diameter as a function of viscosity and found a logarithmic relation for these quantities as is displayed in Figure 9(b). Notice that these fibers were obtained with very low feed rates for which we found the production more stable.

3.3. Polymer Solution Feed Rate

A solution of PEO with an average molecular mass of 900 kg/mol and a concentration of 4 wt% was used. The needle-collector distance was set to 20 cm and 8 kV were applied to the needle while the collector was kept grounded. In Figure 10, SEM images of the fibers obtained for 3 different feed rates are displayed. The mean fiber diameters measured were (209 ± 49) nm for the feed rate of 0.05 ml/h, (234 ± 38) nm for 0.1 ml/h and (303 ± 70) nm for 0.2 ml/h. From the plot of Figure 11 we see that the mean fiber diameter increases linearly with the polymer solution feed rate.

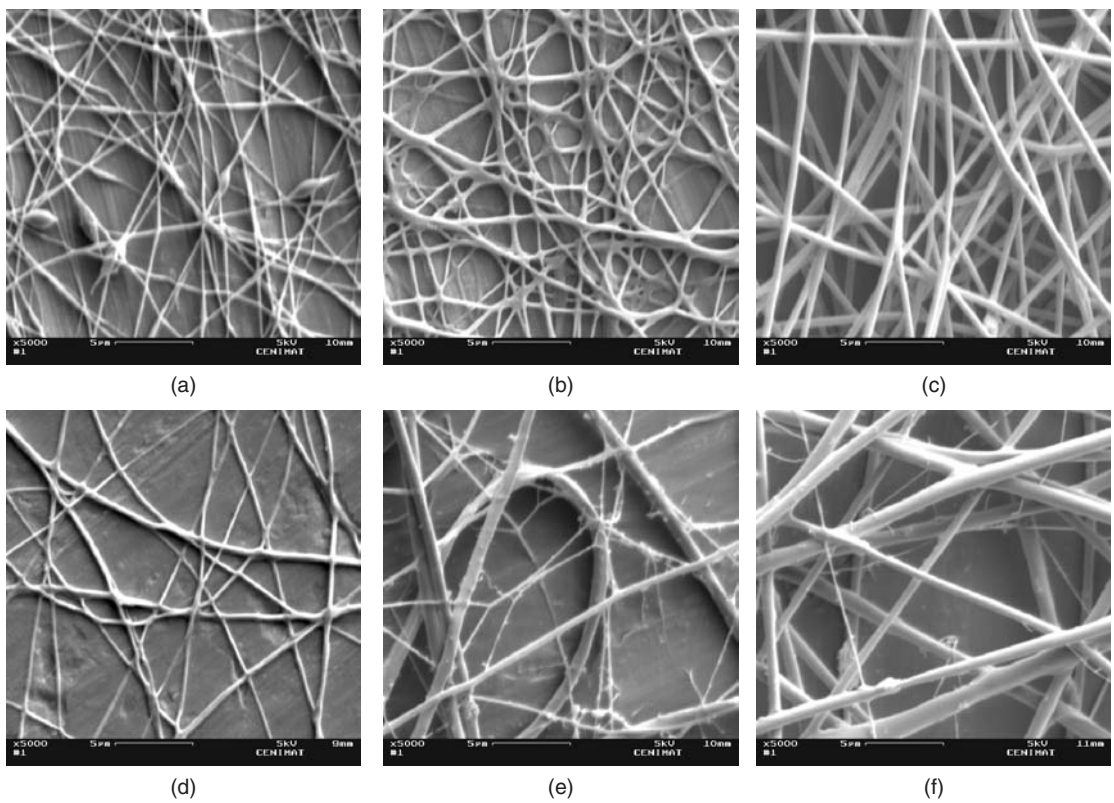

Fig. 8. SEM images of electrospun fibers processed from PEO of different molecular masses: (a) 400 kg/mol, (b) 900 kg/mol, (c) 2000 kg/mol (4 wt%), (d) 2000 kg/mol (2 wt%), (e) 5000 kg/mol and (f) 8000 kg/mol.

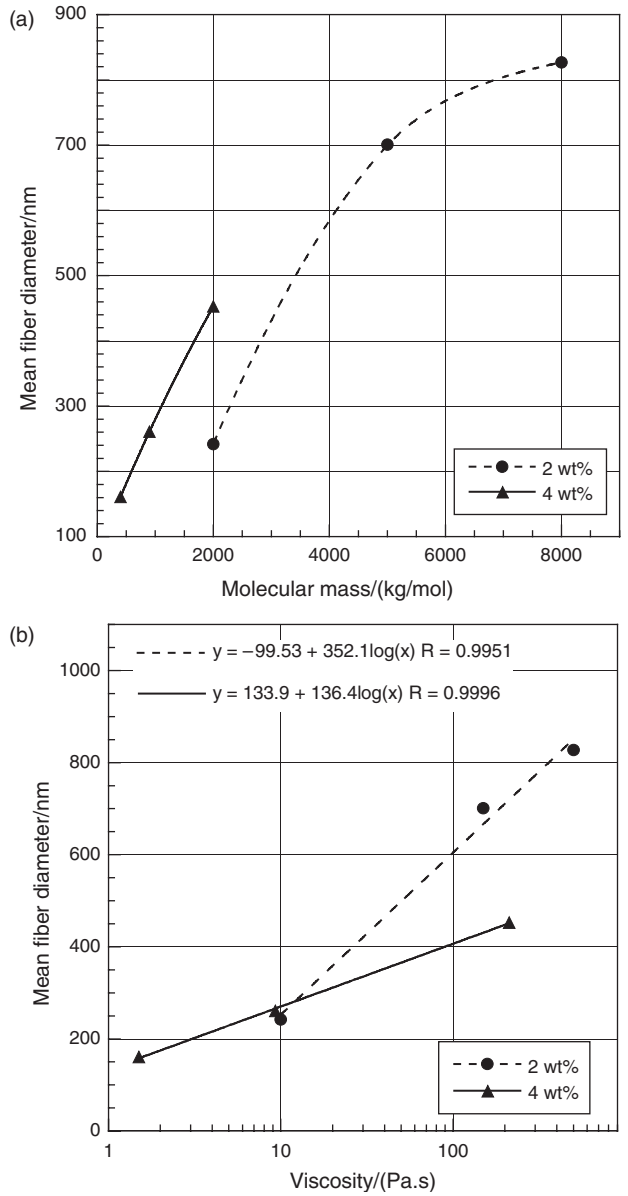

Fig. 9. Mean fiber diameter as a function of: (a) molecular mass (lines are guides to the eye), (b) viscosity (lines are logarithmic fits).

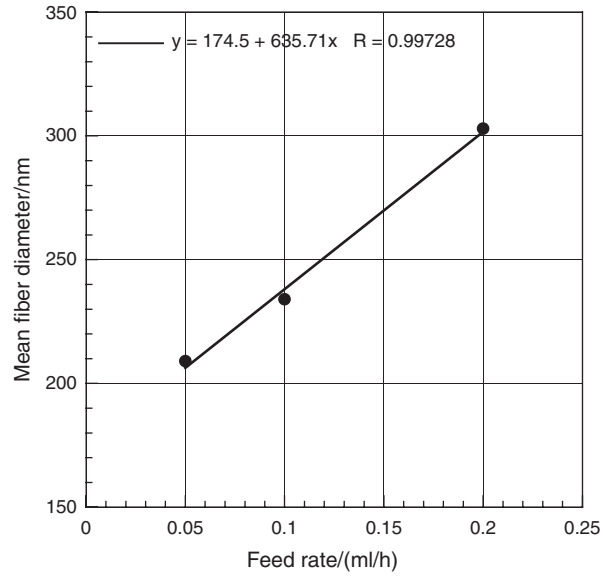

Fig. 11. Mean fiber diameter as a function of the feed rate. Solid line is a linear fit to experimental data.

3.4. Needle Tip-Collector Distance

The PEO solution used was the same as the one for the feed rate study: an average molecular mass of 900 kg/mol and a concentration of 4 wt%. The feed rate was fixed at 0.1 ml/h and the distance from the tip of the needle to the collector was varied from 15 cm to 35 cm. The morphology of the fibers was evaluated from the SEM images of Figure 12.

For the shortest distance used (15 cm) the fibers merge at their intersections due to the incomplete evaporation of the solvent before the jet reaches the collector. For the other 4 distances used, the fibers look much alike and the mean fiber diameter increases only slightly with the distance to the collector, as can be seen in the plot of Figure 13.

Increasing the needle-collector distance, while the potential applied to the needle is constant, has two effects of opposing consequences on fiber diameter. First we note

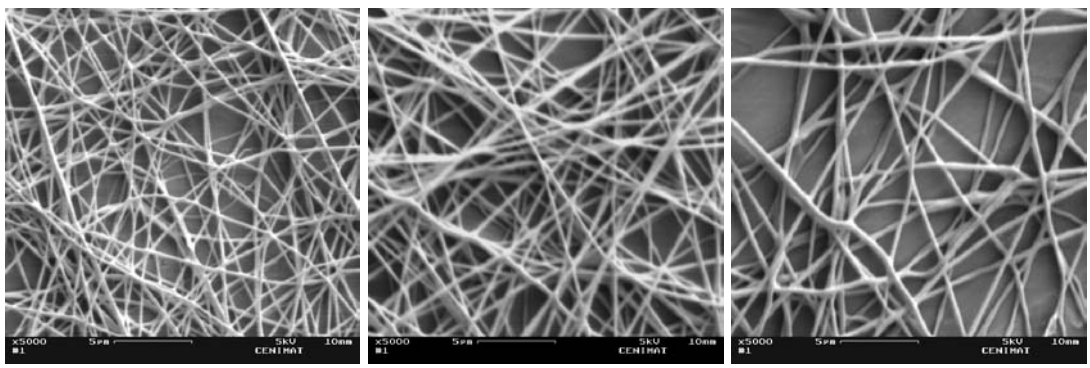

Fig. 10. Fibers electrospun at different feed rates: (a) 0.05 ml/h, (b) 0.1 ml/h, (c) 0.2 ml/h.

RESEARCH ARTICLE

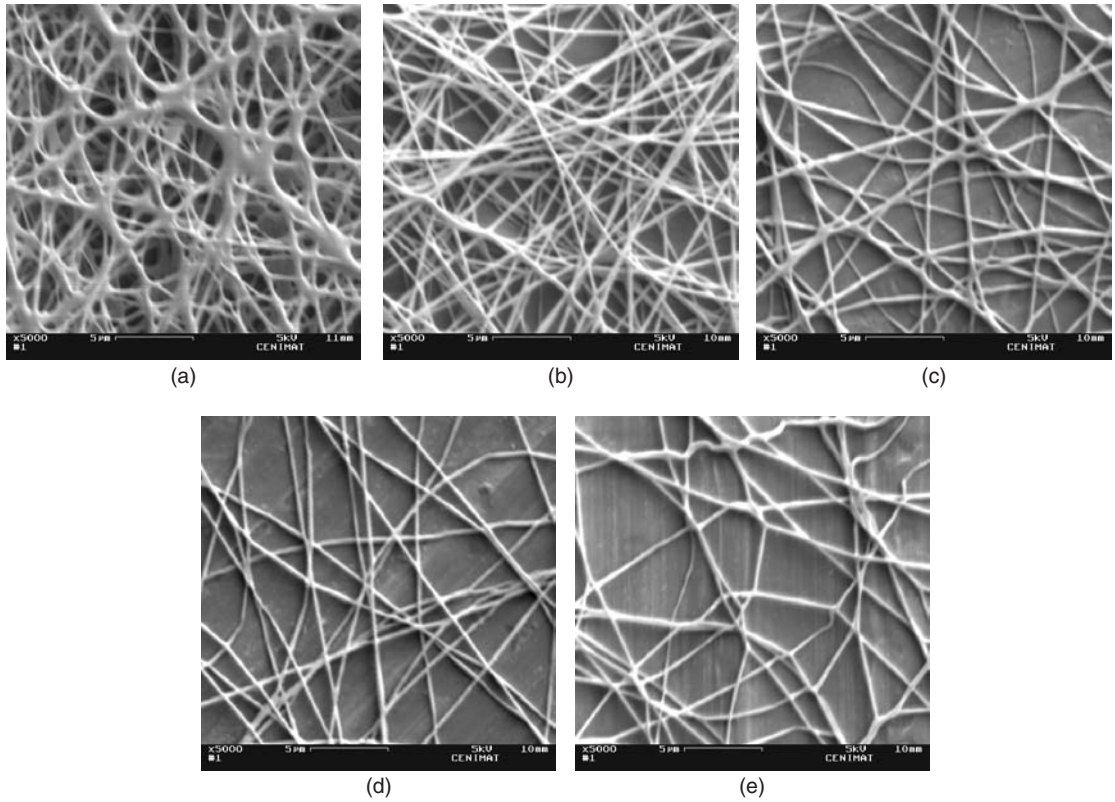

Fig. 12. Fibers electrospun for different needle tip-collector distances: (a) 15 cm, (b) 20 cm, (c) 25 cm, (d) 30 cm, (e) 35 cm.

that stretching of the fibers is influenced by the rate of solvent evaporation. As the solvent evaporates, the viscosity of the fibers increases and the viscoelastic forces within the fibers resist further stretching. The merging of the fibers observed in the 15 cm distance case is indicative of an incomplete solvent evaporation. Since this effect is not seen for longer distances, we conclude that solvent evaporation is mostly complete by the time the fibers reach the collector. Now, when the solvent evaporates completely, the fibers are morphologically "frozen" and no more stretching occurs, even if the fibers are still in the air, traveling towards the collector, charged and subjected to the electric field. Thus, any stretching of the fibers must occur before the viscoelastic forces become dominant and prevent further stretching. Coming back to the relationship between fiber diameter and needle-collector distance. On the one side, the electric field in which the fibers travel decreases with increasing distance and this leads to a smaller stretching force on the fibers, leading to thicker fibers. On the other side, a longer distance means a longer flight time and the possibility of an increased stretching, leading to thinner fibers. The results we obtained, plotted in Figure 13, show an increase of fiber diameter with needle-collector distance and are indicative that the main factor influencing fiber diameter is the decrease of the stretching associated a weaker electric field. The production of thinner fibers is, therefore, associated with stronger electric fields, other parameters kept constant.

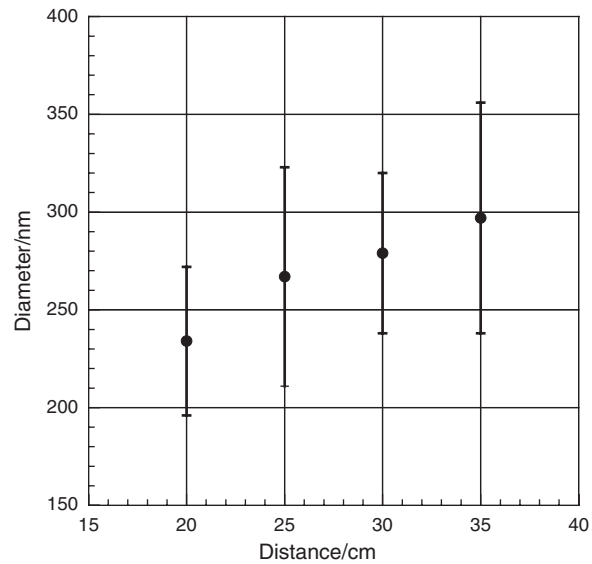

Fig. 13. Fiber diameter as a function of the distance from the tip of the needle to the collector. The dots represent mean values and the bars indicate the standard deviation of the fiber diameters.

3.5. Potential Difference Between the Needle and the Collector

Different values of the high voltage applied to the needle and ring were taken keeping the tip to collector distance and feed rate both fixed. The potential applied to

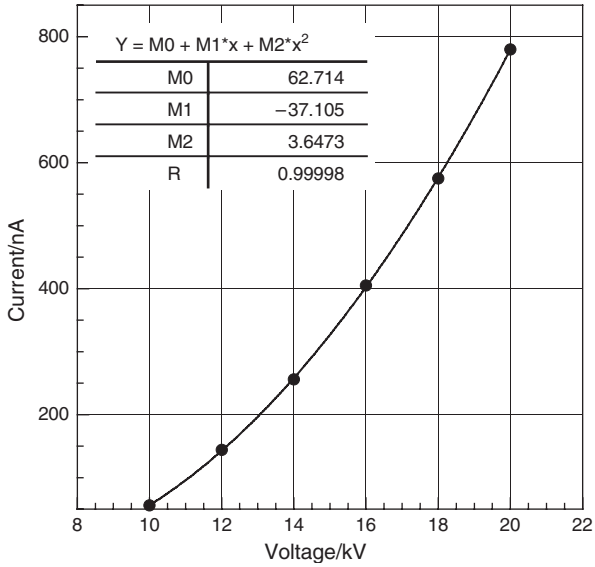

Fig. 14. Current from the collector to the ground as a function of the potential applied to the needle and ring.

the needle determines the charging of the polymer jet and the accelerating electric field in the jet travel region. We measured the discharging current of the collected polymer with a Keithley 617 electrometer connected between the aluminum foil and the ground. Plot of Figure 14 shows an increase of this current with the applied potential for the electrospinning of a 4 wt% solution of 2000 kg/mol PEO and Figure 15 some of the corresponding fibers.

While the formation of thinner fibers is favored by a highly charged jet (a higher electrostatic repulsion produces a higher jet elongation),[12] a shorter travel time due to a high electrostatic acceleration (high field acting on a high charge) results in an incomplete evaporation of the solvent and in the appearance of merged fibers in the collector as is evidenced from Figure 15.

If the collector is grounded and only the needle is polarized it is not possible to control the electric field and the charging of the polymer independently. However, if the potentials applied to the collector and to the needle change while their difference is kept constant, the electric

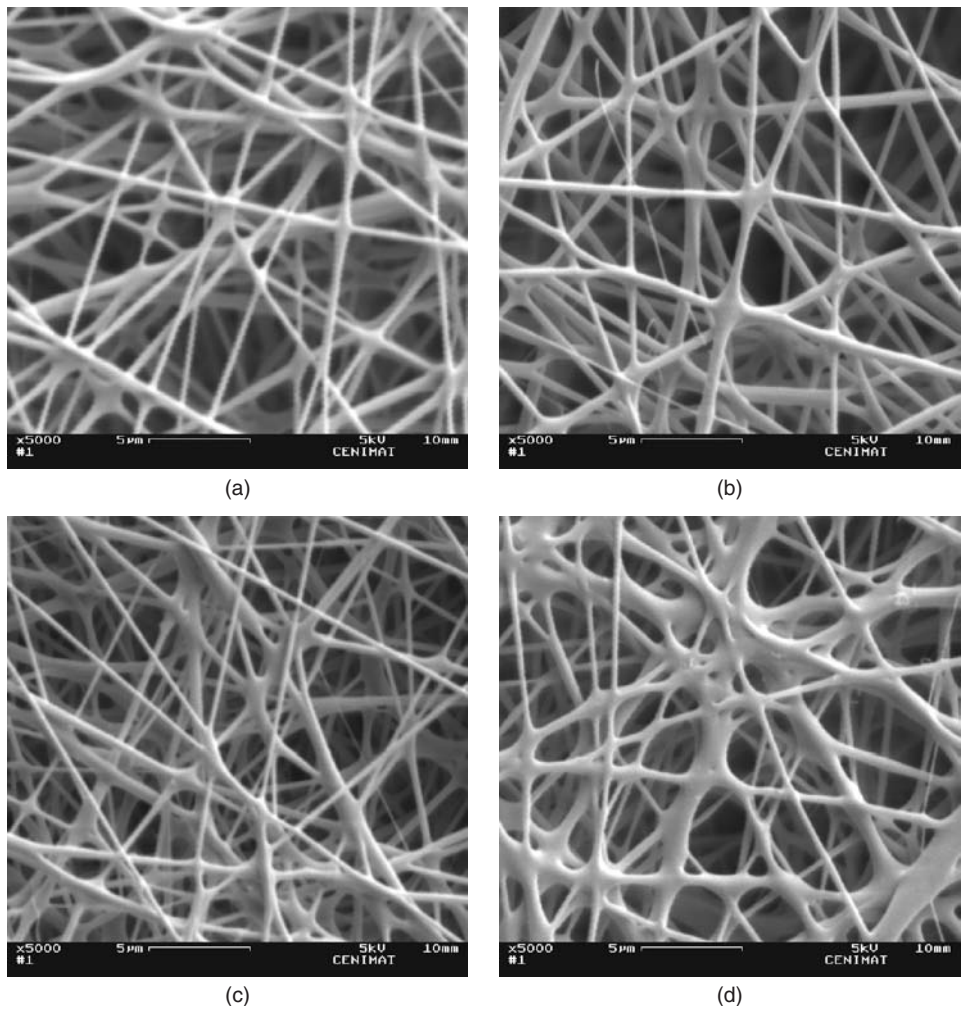

Fig. 15. Fibers electrospun for different potentials applied to the needle: (a) 12 kV, (b) 14 kV, (c) 16 kV and (d) 18 kV. Tip to collector distance was fixed at 25 cm and the feed rate was 0.1 ml/h.

RESEARCH ARTICLE

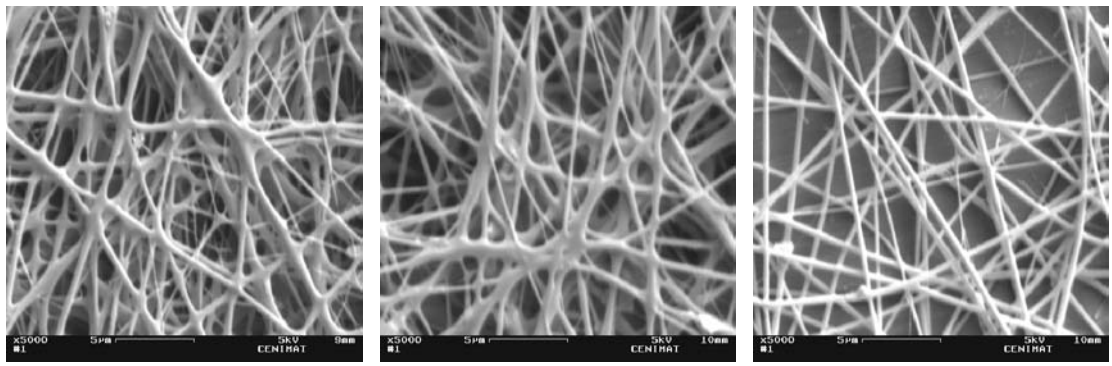

(a) (b) (c)

Fig. 16. Fibers electrospun for different potentials applied to the collector and needle keeping the difference between them fixed. Collector-needle potentials referred to the ground were: (a) 0:15 kV, (b) −5:10 kV and (c) 5:20 kV.

field does not change but the charging of the polymer varies. We studied the influence of this situation on the morphology of the fibers and found an interesting effect. Figure 16 shows fibers electrospun from the 4 wt% solution of PEO of 2000 kg/mol at a feed rate of 0.05 ml/h with the collector at a distance of 25 cm from the needle. The potential difference between the needle and the collector was kept at 15 kV but different potentials were applied: the collector is either grounded, negative or positive. When the collector was grounded and the needle at 15 kV (Fig. 16(a)), the fibers show some merging, again suggesting that solvent evaporation could not complete due to a too short flight time. When the collector was at −5 kV and the needle at 10 kV (Fig. 16(b)), the situation appears to worsen slightly. Less charging of the polymer solution results in this case in less auto-repulsion and again a too short flight time not allowing for a complete solvent evaporation. The situation changed markedly when the collector was at 5 kV and the needle at 20 kV. The increased charging of the polymer appears to favor the formation of defect free fibers (Fig. 16(c)). More charge on the polymer implies a higher acceleration due to the electric field and thus a smaller flight time. This effect alone should contribute to fiber merging. However, a more charged polymer also implies more auto-repulsion and this leads to more stretching, more surface area, higher solvent evaporation rate, more whipping and bending (this may cause either, or both, longer flight time and flight path). In the end, the sum of all these effects is a nanofiber mat with more uniform and defect free fibers, as can be seen in Figure 16(c).

4. CONCLUSIONS

We assembled a new electrospinning apparatus and used poly(ethylene oxide) as a model polymer to perform a systematic study on the influence of solution and processing parameters on the morphological properties of electrospun nanofibers. Solution parameters studied were polymer concentration and molecular mass. The solvent used, 60 wt% water, 40 wt% ethanol, was the same throughout the study. Processing parameters analyzed were: solution feed rate, needle tip-collector distance and electrostatic potential difference between the needle and collector. Whenever a parameter was varied, all others were kept constant.

The viscosities of the solutions used in the studies were measured and found to increase exponentially with solution concentration (for a given molecular mass) and according to a power law as a function of the molecular mass.

The polymer concentration was seen to play a decisive role in the outcome of the electrospinning process. For the lower molecular mass we used (400 kg/mol) a low polymer concentration (4 wt%) leads to the formation of beaded fibers. As the concentration increases fibers of bigger diameters appear, due to the increase of the viscosity of the solution. An intermediate concentration (6 wt%) resulted in fibers with a diameter distribution of mean 258 nm experimental standard deviation of 53 nm. At high concentration (8 wt%) a bimodal size distribution appeared. This was attributed to the appearance of secondary jets originated during splay events which were observed to occur along the linear region of the main jet. At even higher concentration (10 wt%) the jet only initiated when a higher potential was applied to the needle. In this situation the fibers were deposited in three different regions. The central region, where the fibers were more irregular, results from electrospinning a single jet originating at a drop present at the tip of the needle. This single jet would eventually split in two jets due to the high electrostatic repulsion associated with the high potential applied to the needle. The two jets also repelled each other and lead to a stable deposition in opposite sides of the central region. Fibers in these outer regions have smaller diameters and present less defects than those in the central region. The two jets would eventually revert to a single jet.

The polymer molecular mass was seen to have a direct influence on fiber morphology. Fiber diameter increases with average molecular mass and exhibits a logarithmic dependency on the corresponding solution viscosities. The

4 wt% solution of 2000 kg/mol PEO yielded the most regular fibers. Splay events are more likely to occur for the higher molecular masses.

As with an increase of the solution feed rate more polymer is pushed through the needle, fiber diameter also increases. For the feed rates used this dependency was found to be linear.

An increase in the needle-collector distance means a greater distance to be covered by the polymer before reaching the collector and a decrease in the electric field strength. Both effects contribute to an increase in the flight time, which should favor a more pronounced stretching of the fibers due to the electrostatic repulsion of the charged jet. However, solvent evaporation leads to a local increase of polymer concentration and viscosity was seen to increase exponentially with polymer concentration. The viscoelastic forces increase accordingly and eventually prevent further stretching. In this way the fiber diameter increases with the needle-collector distance, a result which could seem strange at first glance. As far as we know this argument based on the variation of the solution viscosity during the flight time is presented for the first time to explain the increase of the fiber diameter with the needle-collector distance.

Varying the high voltage applied to the needle keeping the collector grounded increases the charging of the polymer jet and decreases the jet travel time towards the collector due to a stronger electrostatic force. As a consequence the electrical current flowing between the collector and the ground increases quadratically with the needle voltage. We showed that the decrease in the jet travel time could be responsible for the incomplete solvent evaporation that makes merged fibers appear as the potential is increased.

It is possible to control independently the charging of the polymer and the electric field strength if a voltage is applied to the collector and the distance and potential difference between the needle and the collector are kept constant. The increased electrostatic repulsion associated with an increase of the high voltage applied to the needle lead to the disappearance of merged fibers and a more consistent nanofiber mat.

References and Notes

1. S. Ramakrishna, K. Fujihara, W. E. Teo, T. C. Lim, and Z. Ma, An Introduction to Electrospinning and Nanofibers, World Scientific, Singapore (**2005**).
2. W. E. Teo and S. Ramakrishna, *Nanotechnology* 17, R89 (**2006**).
3. T. B. Bini, S. J. Gao, T. C. Tan, S. Wang, A. Lim, L. B. Hai, and S. Ramakrishna, *Nanotechnology* 15, 1459 (**2004**).
4. S. Kidoaki, I. K. Kwon, and T. Matsuda, *Biomaterials* 26, 37 (**2005**).
5. J. Lannutti, D. Reneker, T. Ma, D. Tomasko, and D. Farson, *Mater. Sci. Eng. C* 27, 504 (**2007**).
6. M. Khil, D. Cha, H. Kim, I. Kim, and N. Bhattarai, *J. Biomed. Mater. Res.* 67B, 675 (**2003**).
7. J. Venugopal, Y. Zhang, and S. Ramakrishna, *Artif. Organs* 30, 440 (**2006**).
8. S. Bhattarai, N. Bhattarai, H. Yic, P. Hwang, D. Chad, and H. Kim, *Biomaterials* 25, 2595 (**2004**).
9. J. Zeng, X. Xu, X. Chen, Q. Liang, X. Bian, L. Yang, and X. Jing, *J. Control. Release* 92, 227 (**2003**).
10. G. Verreck, I. Chun, J. Rosenblatt, J. Peeters, A. van Dijck, J. Mensch, M. Noppe, and M. E. Brewster, *J. Control Release* 92, 349 (**2003**).
11. K. Kim, Y. K. Luuc, C. Chang, D. Fang, B. S. Hsiao, B. Chua, and H. Hadjiargyrou, *J. Control Release* 98, 47 (**2004**).
12. H. Fong, I. Chun, and D. H. Reneker, *Polymer* 40, 4585 (**1999**).
13. J. M. Deitzel, J. Kleinmeyer, D. Harris, and N. C. B. Tan, *Polymer* 42, 261 (**2001**).
14. J. M. Deitzel, J. Kleinmeyer, J. K. Hirvonen, and N. C. B. Tan, *Polymer* 42, 8163 (**2001**).
15. W. K. Son, J. H. Youk, T. S. Lee, and W. H. Park, *Polymer* 45, 2959 (**2004**).
16. G. Taylor, *Proc. R. Soc. London A* 280, 383 (**1964**).
17. T. A. Kowalewski, S. Blonski, and S. Barral, *Bull. Pol. Ac.: Tech.* 53, 385 (**2005**).
18. J. Zeng, X. Chen, X. Xu, Q. Liang, X. Bian, L. Yang, and X. Jing, *J. Appl. Polym. Sci.* 89, 1085 (**2003**).

Received: 6 August 2007. Accepted: 29 November 2007.

RESEARCH ARTICLE